Ca–Cu looping process for CO2 capture from a power plant and its comparison with Ca-looping, oxy-combustion and amine-based CO2 capture processes

International Journal of Greenhouse Gas Control 43 (2015) 198–212

Contents lists available at ScienceDirect

International Journal of Greenhouse Gas Control

journal homepage: www.elsevier.com/locate/ijggc

Ca–Cu looping process for CO_2 capture from a power plant and its comparison with Ca-looping, oxy-combustion and amine-based CO_2 capture processes

Dursun Can Ozcan[a,*], Arturo Macchi[b], Dennis Y. Lu[c], Agnieszka M. Kierzkowska[d], Hyungwoong Ahn[a], Christoph R. Müller[d], Stefano Brandani[a]

[a] Scottish Carbon Capture and Storage Centre, School of Engineering, University of Edinburgh, Mayfield Road, Edinburgh EH9 3JL, UK
[b] Department of Chemical and Biological Engineering, University of Ottawa, Ottawa, Ontario K1N 6N5, Canada
[c] Natural Resources Canada, CanmetENERGY, 1 Haanel Drive, Ottawa, Ontario K1A 1M1, Canada
[d] Laboratory of Energy Science and Engineering, ETH Zurich, Leonhardstrasse 27, 8092 Zurich, Switzerland

ARTICLE INFO

Article history:
Received 24 April 2015
Received in revised form 19 October 2015
Accepted 27 October 2015

Keywords:
CO_2 capture
Power plant
Calcium looping process
Chemical looping combustion
Integrated Ca–Cu looping process

ABSTRACT

This study reports the technical performance of an advanced configuration of the calcium looping (Ca-looping) process, called Ca–Cu looping, for the reduction of CO_2 emissions from a subcritical CFB power plant with a net output of 250 MW_e. In this new process concept, the thermal power requirement in the calciner is satisfied using a chemical looping combustion cycle. Thus, the power consumption associated with the air separation unit that is required in the conventional Ca-looping process scheme can be eliminated. The reference power plant has also been modified to integrate oxy-combustion, Ca-looping and amine scrubbing technologies for comparison. The fully integrated process flowsheets have been simulated using Honeywell's UniSim Design Suit R400. For a more accurate prediction of the CO_2 capture efficiency in the carbonator of the Ca–Cu looping process, the experimentally obtained cyclic activity of a novel copper-functionalised, calcium-based composite sorbent has been implemented yielding a rigorous carbonator model. The process simulations also include a comprehensive analysis of the CO_2 compression and purification unit as well as a heat exchanger network optimized using pinch analysis for the recovery of excess heat from the high temperature gas and solid streams available in the Ca-looping and Ca–Cu looping processes. Compared to the energy penalty of 10.5 percentage points for a conventional amine scrubbing configuration, the Ca–Cu looping process evaluated in this study achieves the same overall CO_2 capture efficiency with a significantly reduced energy penalty of 3.5 percentage points; the lowest value for all CO_2 capture architectures assessed here.

1. Introduction

Global CO_2 emissions totalled 34.5 Gt in 2012 (Olivier et al., 2013) and are predicted to increase further, reaching 40.2 Gt by 2030 (IEA, 2009a). The National Oceanic and Atmospheric Administration (NOAA)/Earth System Research Laboratory (Dlugokencky and Tans, 2014) reported that the global CO_2 concentration reached 400 ppm in 2013, which is a 24% increase when compared to 1958. According to the latest report of the Intergovernmental Panel on Climate Change (IPCC, 2013), it is highly likely (95% confidence) that humans are the primary cause for global warming. The world energy demand is envisioned to increase by 40% from 2007 to 2030 (IEA, 2009b) while fossil fuels will remain as the major source for energy conversion. The increasing energy demand will, therefore, increase further the CO_2 emissions from fossil fuel combustion unless more efficient and cleaner energy conversion technologies are introduced.

As stated in the Climate Change Act (UKP, 2008), the UK aims for an >80% reduction of its CO_2 emissions by 2050 when compared to value of 1990 while Canada aims to reduce greenhouse gas emissions by 17% compared to its 2005 level by 2050 (EC, 2013a). Carbon capture and storage (CCS) is a promising and emerging way of reducing CO_2 emissions from fossil-fuel fired power stations and industrial processes such as cement, iron and steel production plants (DOE, 1999). The IEA (2010) estimates that by 2050, CCS can contribute to a decrease on global CO_2 emission by approximately 19%. According to the economic analysis by Rao and Rubin (2002),

* Corresponding author. Current address: TUBITAK, Tunus Caddesi No.: 80, Kavaklıdere, Ankara 06100, Turkey.
E-mail address: can.ozcan@tubitak.gov.tr (D.C. Ozcan).

http://dx.doi.org/10.1016/j.ijggc.2015.10.021
1750-5836/

the CO_2 capture step in CCS accounts for 75–85% of the overall cost associated with CCS. Therefore, it is important to develop efficient and cost-effective CO_2 capture technologies.

Among various CO_2 capture technologies, absorption, oxy-combustion and calcium looping (Ca-looping) processes have received substantial interest. In this regard, amine scrubbing is the most mature technology for post-combustion CO_2 capture. The most widely applied amine-based sorbent is monoethanolamine (MEA). It has been used for over 80 years (Bandyopadhyay, 2011) and several techno-economic studies are available for this process (EPRI, 2009; Finkenrath, 2011). In the oxy-combustion process, instead of air, almost pure oxygen (≥95 mol%) is used for combustion yielding, after the condensation of steam, an almost pure CO_2 stream (>90 mol%) in the flue gas (Jared et al., 2010). The Babcock & Wilcox Company has demonstrated the oxy-combustion concept on the 30 MW_{th} scale (McCauley et al., 2009).

The Ca-looping process, based on a reversible reaction between CaO and CO_2, is a promising and effective way to capture CO_2 from large point sources. It has attracted significant interest owing to the use of cheap and widely available sorbents (CaO). The Ca-looping technology has been tested at different scales including a 1.9 MW_{th} pilot at ITRI, Taiwan (Chang et al., 2013), a 1.7 MW_{th} pilot in La Pereda, Spain (Arias et al., 2013), a 1 MW_{th} pilot plant at TU Darmstadt, Germany (Kremer et al., 2013) and a 75 kW_{th} dual fluidized bed system in CanmetENERGY, Canada (Lu et al., 2008). The post-combustion Ca-looping process was first proposed by Shimizu et al. (1999) and typically comprises two interconnected circulating fluidized bed (CFB) reactors. In the first reactor, called carbonator, CO_2 from the flue gases reacts with CaO at 600–750 °C. The product, $CaCO_3$ is regenerated back to CaO and CO_2 in the calciner at 870–950 °C according to reaction (1):

$$CaO + CO_2 \leftrightarrow CaCO_3 \quad (\Delta H_{650\,^\circ C} = -171\ kJ/mol) \tag{1}$$

The heat requirement in the calciner is provided by the oxy-combustion of additional fuel (Romeo et al., 2008). Despite the fact that additional heat is required for the calciner, one of the advantages of this system is the possibility to recover surplus heat from hot gas and solid streams leaving the reactors as well as the exothermic carbonation reaction. This additional heat can be used to drive a steam cycle to generate electricity, reducing in turn, the energy penalty of the CO_2 capture system. A disadvantage of CaO-based sorbent is the decreasing CO_2 uptake with the number of carbonation and calcination cycles primarily due to material sintering (Curran et al., 1967). Although substantial research efforts are currently being undertaken to reduce the decay in CaO reactivity (Lu et al., 2006; Fennell et al., 2007; Gonzalez et al., 2011; Manovic and Anthony, 2011a; Ozcan et al., 2011; Kierzkowska et al., 2013), some fraction of the spent sorbent has to be continuously replaced by fresh sorbents. If the spent sorbent from the Ca-looping process can be used as a raw material for cement manufacture (Dean et al., 2011a; Telesca et al., 2014), the CO_2 emission due to the calcination of limestone in the cement process can be eliminated (Dean et al., 2011b; Rodriguez et al., 2012; Ozcan et al., 2013).

One of the greatest challenges associated with the Ca-looping process is the need of an energy intensive air separation unit (ASU) to ensure the production of a stream of high purity CO_2 in the calciner. The addition of an ASU also increases the total capital requirement of the plant. A novel alternative for the transfer of pure oxygen into the calciner was proposed recently by Abanades and Murillo (2009). In their work, a chemical looping combustion (CLC) system was coupled with a Ca-looping process (hereinafter called Ca–Cu looping process) to provide heat to the calciner by the exothermic reduction of a metal oxide (CuO). CLC is a fairly recent CO_2 capture concept, allowing the inherent production of pure CO_2 (after the condensation of steam) (Ishida and Jin, 1994; Lyon and Cole, 2000; Imtiaz et al., 2013). In contrast to the conventional combustion process, oxygen for the combustion reaction is provided by the reduction of metal oxides according to reaction (2):

$$(2n+m)Me_xO_y + C_nH_{2m} \rightarrow (2n+m)Me_xO_{y-1} + mH_2O + nCO_2 \tag{2}$$

Some well-known oxygen carriers are the oxides of Ni, Cu, Fe and Mn commonly supported by inert materials such as Al_2O_3, MgO and TiO_2 (Hossain and de Lasa, 2008). The exit gas stream from the fuel reactor contains CO_2 and H_2O, which can then be condensed to obtain pure stream of CO_2. The reduced metal oxide is re-oxidized with air according to reaction (3):

$$Me_xO_{y-1} + 1/2O_2 \rightarrow Me_xO_y \tag{3}$$

In theory, the oxidation reaction is always exothermic but the reduction reaction can be either endothermic or exothermic depending on the metal oxide. In the case of Ca–Cu looping process, CuO is one of the most promising oxygen carriers owing to its exothermic reduction with hydrocarbon based fuels and its high oxygen carrying capacity (Abanades and Murillo, 2009; Abanades et al., 2010; Manovic and Anthony, 2011b; Manovic et al., 2011c).

To date, a variety of experimental demonstrations using CuO/CaO sorbents have been reported for pre-combustion and post-combustion CO_2 capture (Manovic and Anthony, 2011d; Kierzkowska and Müller, 2012). Due to the low melting point of CuO (1085 °C) and the activity loss of CaO due to sintering, Al_2O_3 is often added as a support. Abanades et al. (2010), Fernandez et al. (2012) and Martinez et al. (2014) investigated this process for hydrogen production and/or electricity generation from natural gas by sorption enhanced reforming. Abanades and Murillo (2009) and Manovic and Anthony (2011d) proposed different process schemes for its practical implementation for the post-combustion applications. Kierzkowska and Müller (2012) reported that a Ca–Cu composite without any inert support can be manufactured by using a co-precipitation technique. Later this group indicated that sol-gel derived, calcium-based, copper-functionalised CO_2 sorbents possess excellent oxygen-carrying and stable CO_2 uptake capacities (Kierzkowska and Müller, 2013). The performance of MgO supported CaO/CuO (Qin et al., 2012) as well as the effects of thermal pre-treatment of CuO and steam addition on the sorbent performance was also examined (Qin et al., 2013).

Despite the potential importance of the Ca–Cu looping concept to reduce the energy consumption of the conventional Ca-looping process, this study will be the first to report its technical applicability as a post-combustion technology. Here, we also report the experimental performance of a novel copper-functionalised, calcium-based composite sorbent that is used as a sorbent and oxygen carrier in the Ca–Cu looping process. Furthermore, the comparison of the Ca–Cu looping process with the oxy-combustion, Ca-looping, and amine scrubbing processes in terms of their process energy efficiencies is presented.

2. Reference CFB power plant

Coal-fired power plants generated 40% of the world's electricity with a global capacity of 1627 GW in 2010, and 75% of this global capacity was from subcritical power plants while the remaining 22% and 3% were from supercritical and ultra-supercritical power plants, respectively (IEA, 2012; Caldecott et al., 2015). Thus, since the subcritical power plants still dominate coal-fired power generation, a subcritical CFB power plant with a nominal net output of 250 MW_e (DOE, 2003) is selected to be reference power plant in this study. The simplified process diagram of the reference power plant including a subcritical steam cycle is shown in Fig. 1 (DOE, 2003, 2007). It burns Genesee coal at full load and uses air as the oxidant for combustion while neglecting CO_2 capture from the flue gas stream. The ultimate, proximate and calorific analyses of Genesee coal are given in Table 1. The excess air ratio for the combustion

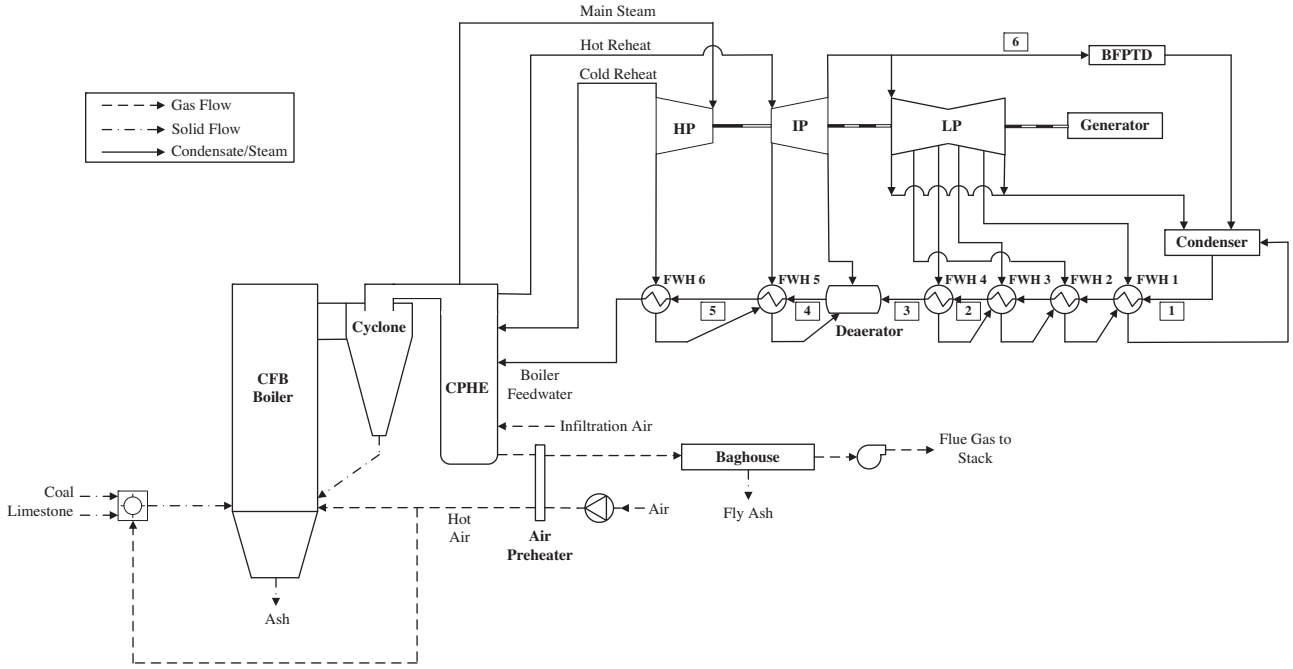

Fig. 1. Schematic diagram of the reference power plant (DOE, 2003, 2007). CFB: circulating fluidized bed, CPHE: convection pass heat exchangers, BFPTD: boiler feed pump turbine drives, HP: high pressure turbine, IP: intermediate pressure turbine, LP: low pressure turbine, FWH: feedwater heater.

is set to 15%, and complete combustion of the fuel is assumed. The steam cycle provides a main steam at 566 °C and 166.5 bar and a reheat at 566 °C and 38.3 bar. A more detailed schematic diagram of the steam cycle and stream properties are given in a previous study (Ozcan et al., 2014) and in the relevant reference (DOE, 2007). The low peak flame temperature in the CFB boiler minimizes the formation of thermal-NO_x, and the environmental limits of NO_x emissions can be met without an additional DeNO$_x$ system (IEAGHG, 2009). The addition of limestone in the boiler allows the capture of SO_2 from the combustion. By setting the Ca/S ratio to 2.5, a SO_2 capture efficiency of 90% is assumed (DOE, 2003).

In the reference CFB power plant, coal is fired with preheated air in the boiler. The air is supplied via a fan which increases the pressure by 0.2 bar to overcome the pressure drop in the boiler. The steam cycle consists of a triple-pressure system of high pressure (HP), intermediate pressure (IP) and low pressure (LP) turbines. The condensate leaving the condenser is transported through a series of feedwater heaters (FWHs). Each FWH receives a separate extraction steam from the turbines. The flow rate of infiltration air is assumed to be 2 wt% of that of the flue gas stream from the boiler (DOE, 2003, 2007). The excess heat from the flue gas stream is transferred to the combustion air prior to the baghouse while the final temperature of the preheated air is determined by setting the flue gas temperature to 135 °C to overcome the stack effect (DOE, 2003). The fine particulate matter in the flue gas stream is removed in a baghouse, and the gas stream enters an induced fan to compensate the pressure drop of 0.05 bar before being discharged to the atmosphere (DOE, 2003). Although some part of the power requirements for the plant auxiliaries can be estimated by using process simulations, others such as solid handling, preparation and feed units, and particulate removal system have been calculated by sizing the equipments against the reference values given in the DOE report (DOE, 2003).

Table 1
The ultimate, proximate and calorific analyses of Genesee coal. LHV: lower heating value.

	Genesee coal (wt.%)
Proximate analysis	
Moisture	6.80
Ash	22.04
Volatiles	28.38
Fixed carbon	42.78
Ultimate analysis	
Carbon	54.15
Hydrogen	3.21
Nitrogen	0.78
Sulfur	0.30
Oxygen	12.72
Calorific analysis	
LHV (MJ/kg)	21.67

3. Reference power plant with the Ca–Cu looping process

3.1. Preliminary process analysis

Fig. 2 shows three different solid routes for the Ca–Cu looping process. The solids in the system can be circulated in the following direction: carbonator → calciner (fuel reactor) → air reactor → carbonator (Route 1). In addition, Manovic and Anthony (2011d) proposed two other solid circulation routes, viz. carbonator → calciner → carbonator, labelled as Route 2 and carbonator → air reactor → calciner → carbonator (Route 3). In Route 2, an air reactor is not included since it is assumed that sufficient oxygen is present in the feed flue gas to regenerate the depleted oxygen carrier. Nevertheless, the oxygen content of the power plant flue gas (composition given in Table 2) is not sufficient to oxidize the large amount of Cu to CuO. Therefore, Route 2 is not considered here. Route 3 would be another option, but the main concern here is that the temperature of the air reactor needs to be controlled very precisely to prevent any calcination in this reactor. Furthermore, the operating temperature of the air reactor will be lower than that of the calciner which makes heat transfer from the air reactor to the calciner unfeasible. Hence, in this study only Route 1 is analyzed in detail.

The flue gas stream from the reference power plant is fed to the carbonator for CO_2 capture. The pressure drop in each

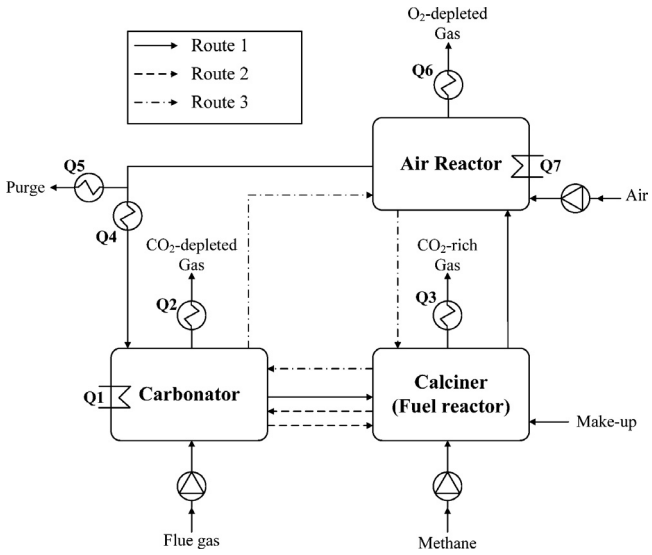

Fig. 2. Schematic diagram of the Ca–Cu looping process including three different solid routes (Manovic and Anthony, 2011d).

Table 2
The composition of the flue gas stream from the reference power plant.

	mol%
CO_2	15.5
O_2	3.2
SO_2	Trace[a]
N_2	74.6
H_2O	6.7
Total	100.0
Molar flow (kg mol/h)	30,253

[a] The SO_2 concentration in the flue gas was calculated to be 32 ppm.

Table 3
Chemical reactions defined in the Ca–Cu looping process simulations.

Reactor	Reaction	$\Delta H_{25\,^\circ C}$ (kJ/mol)
Carbonator	$CaO(s) + CO_2(g) \rightarrow CaCO_3(s)$	−179
Calciner	$4CuO(s) + CH_4(g) \rightarrow 4Cu(s) + CO_2(g) + 2H_2O(g)$	−158
	$CaCO_3(s) \rightarrow CaO(s) + CO_2(g)$	+179
Air reactor	$2Cu(s) + O_2(g) \rightarrow 2CuO(s)$	−320

reactor is assumed to be 0.2 bar, and a fan is located on each inlet gas stream to boost the pressure. Distinct from the reference power plant where the heat recovery from the flue gas stream is limited in order to overcome the stack effect, it is possible to recover further heat from the flue gas stream when it is sent to the carbonator. The temperature of the flue gas stream can be reduced to 85 °C instead of 135 °C considering a minimum temperature difference (MTD) of 20 °C in the air preheater. Such heat transfer allows the generation of more steam at high temperature and increases the gross power capacity of the reference power plant.

It should be noted that the main property of a metal oxide to be employed in the Ca–Cu looping system is an exothermic reduction reaction. In this study, a mixture of $CuO/CaO/Al_2O_3$ has been selected as the sorbent and oxygen carrier (Manovic and Anthony, 2011d; Martinez et al., 2014), and methane with a lower heating value (LHV) of 50 MJ/kg is used as the fuel in the calciner. It should be mentioned that the higher cost of methane compared to that of the coal and the lower power efficiency of burning methane directly compared to a Natural Gas Combined Cycle (NGCC) could be the potential drawbacks of this approach. In this new process concept, CaO captures the CO_2 of the flue gas in the carbonator that operates at 650 °C, whereas the heat requirement for the calcination reaction is satisfied by the exothermic reduction of CuO with methane in the calciner. The Cu leaving the calciner is oxidized back to CuO in the air reactor.

All reactions occurring in the Ca–Cu looping process are given in Table 3. The sum of oxidation and reduction reactions occurring in two different reactors gives the overall methane combustion reaction viz.

$$CH_4(g) + 2O_2(g) \rightarrow CO_2(g) + 2H_2O(g) \quad (\Delta H_{25\,^\circ C} = -798\,\text{kJ/mol}) \tag{4}$$

It should be emphasized that only approximately 20% of the heat of the methane combustion is usable in the calciner while the remaining has to be recovered, at least partially, in the air reactor. Since the main aim of the Ca–Cu looping concept is to provide heat to the calciner with less expense in the air reactor, it is clear that a method of heat transfer from the air reactor to the calciner is necessary in order to prevent excessive thermal power requirement for this CO_2 capture architecture. Rodriguez et al. (2011) proposed the indirect calcination process that uses high temperature solid circulation from a CFB combustor to a fluidized bed calciner to transfer the heat required for limestone calcination. In this process, the combustor operates at a higher temperature than the calciner, and the heat transferred by hot CaO particles satisfies the heat requirement in the calciner. In this manner, the air reactor can be operated at a higher temperature than that of the calciner in Route 1 as presented in Fig. 3. The surplus heat from this reactor, transferred by circulation of hot solid particles, reduces the heat requirement in the calciner. It would also affect the sorbent composition since the required methane and CuO flows both reduce with a decrease in the calciner heat requirement. Therefore, the fraction of CuO in the sorbent can potentially be decreased. Another advantage of this approach would be the elimination of a cooling requirement in the air reactor.

While higher reactor temperatures facilitate heat transfer by reducing solid circulation rates, it is also well-known that an increase in temperature enhances sorbent degradation due to sintering. The operating temperature of the calciner is, therefore, set to 885 °C considering a 15 °C increase when compared to the equilibrium temperature of the calcination–carbonation reaction (Garcia-Labiano et al., 2002). The excess CuO ratio is set to 30% to guarantee complete oxidation of methane in the calciner (Forero et al., 2011). The air reactor temperature is limited to 950 °C. To determine the flow rate of air into this reactor, the molar fraction of O_2 in the O_2-depleted stream from the air reactor is fixed to 3 mol%, and complete oxidation of Cu is assumed in each cycle (de Diego et al., 2004; Garcia-Labiano et al., 2004).

Due to the expected degradation of the CO_2 uptake capacity as a result of the high reactor temperatures, a fraction of the spent sorbent needs to be replaced with fresh sorbent. To capture the CO_2 resulting from the calcination of the fresh sorbent, the new material has to be fed to the calciner. The make-up stream contains not only $CaCO_3$ from limestone but also CuO and Al_2O_3 that leave the system in the purge. To capture the effect of sorbent attrition, it is assumed that 10% of the fresh sorbent leaves the calciner in the gas stream (CO_2-rich gas). If the purge stream is removed from the calciner, the heat released by the oxidation of Cu cannot be recovered. To prevent such heat losses, the purge stream is removed from the air reactor. At this point, it is not clear in the literature how a purge stream containing CaO, CuO and Al_2O_3 can be utilized. However, CaO and Al_2O_3 are raw materials for cement and can be used potentially for

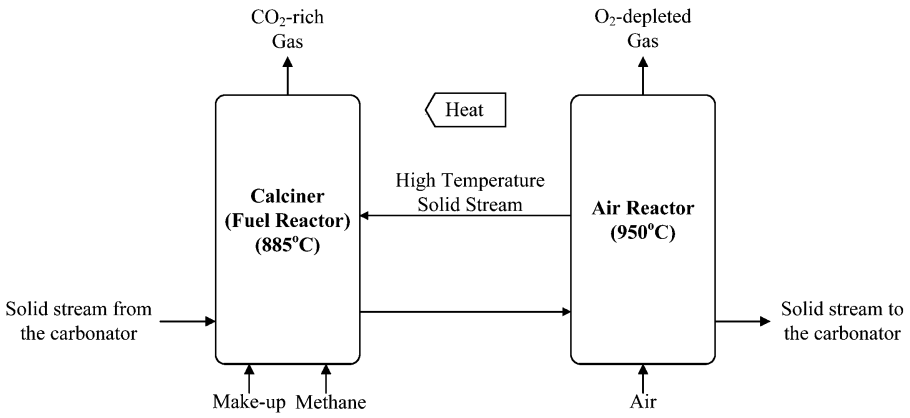

Fig. 3. Application of the indirect calcination process (Rodriguez et al., 2011) into the Ca–Cu looping process (Route 1 in Fig. 2).

the production of cement clinker. Kolovos et al. (2005) indicated that the addition of 1 wt% CuO to the cement raw meal promotes sintering and improves the burnability of the cement raw meal. It would be more appropriate to separate CuO and Al_2O_3 leaving the capture system and reuse them in the make-up stream. However, this option requires a more detailed study and is not considered in the scope of this work.

3.2. Design of CO_2 compression facilities

It should be highlighted that we have set a minimum CO_2 purity of 95 mol% in all CO_2 capture technologies evaluated here. Even though the infiltration air assumption is kept similar to that of the reference power plant in the proposed Ca–Cu looping process, it is possible to reach the targeted purity without a CO_2 purification stage because there is no excess oxygen or other impurities from coal combustion in the CO_2-rich gas stream. To support this argument, the approximate composition of the liquid CO_2-rich gas stream from the Ca–Cu looping process without a CO_2 purification stage is given in Section 7. It is more critical to include the infiltration air assumption in the oxy-firing systems, such as the calciner of Ca-looping process and the combustor of oxy-firing power plant, as it further reduces the CO_2 purity and therefore, reveals the requirement of CO_2 purification stage to reach the targeted purity. Two different CO_2 compression unit configurations are presented in Fig. 4. The first configuration, shown in Fig. 4a, is used for the Ca–Cu looping process and comprises of four compressors with intermediate cooling, followed by a pump. It excludes a CO_2 purification stage. The gas stream is cooled to 35 °C after each compression cycle, and the condensate is separated. Once the CO_2 stream becomes a dense phase after the final compression stage, the pressure of the liquid CO_2 is boosted to the target pressure of 150 bar via a pump. The second configuration, presented in Fig. 4b, includes a CO_2 purification stage (Xu et al., 2012). This configuration consists of a compressor train that is similar to the one presented in Fig. 4a excluding the final compression stage and pump, a two-stage refrigeration system using the coolant R502 as suggested in Xu et al. (2012), and a two-stage separation and energy recovery system. In the first separation stage, the feed gas stream is compressed to 24 bar and cooled to −35 °C, while the remaining flue gas is further compressed to 54 bar and again cooled to −35 °C in the second stage. The separated CO_2 in the liquid phase is then

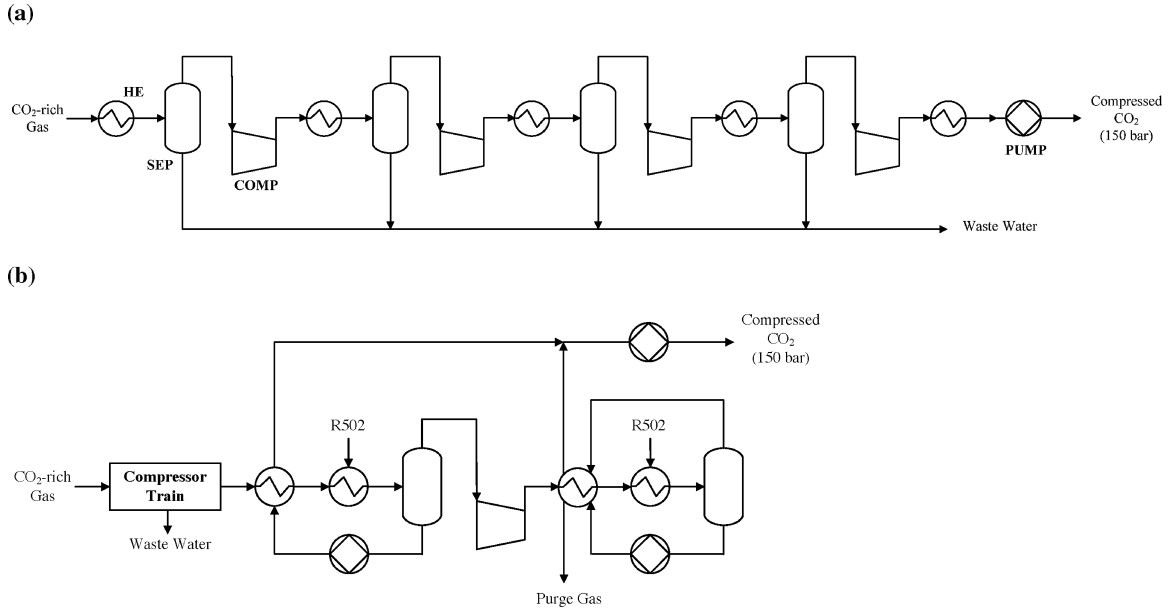

Fig. 4. Process scheme of the CO_2 compression unit without (a) and with (b) a CO_2 purification stage (Xu et al., 2012). HE: heat exchanger, SEP: separator, COMP: CO_2 compressor, R502 as a coolant in the refrigeration cycle.

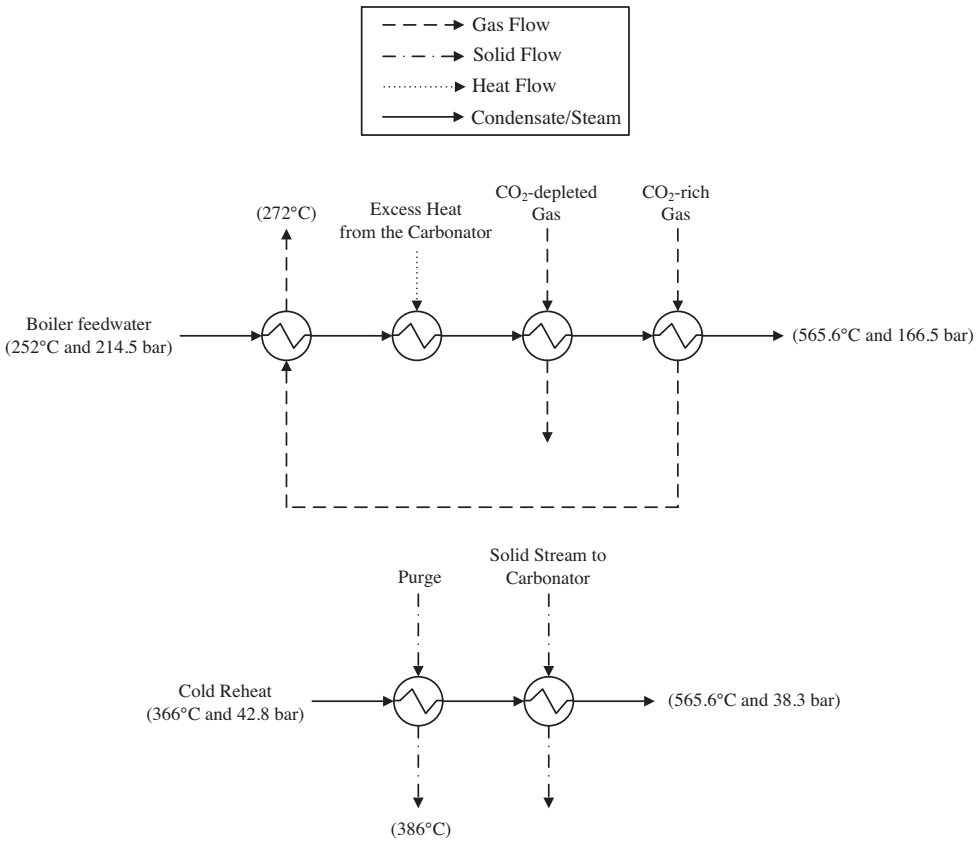

Fig. 5. Proposed heat exchanger network (HEN) design for the recovery of excess heat available in the Ca–Cu looping process.

compressed to 150 bar. To estimate the power requirement for the CO_2 compression and purification unit (CPU), the coefficient of performance for the refrigeration cycle using R502 as a coolant is taken as 1.36 (Xu et al., 2012), and the adiabatic efficiency of the compressors, pumps and expanders is estimated to be 80% (Merkel et al., 2010).

3.3. Carbonator model and experimental data for the Ca–Cu sorbent

The carbonator model employed to predict the carbonation efficiency in this study was developed by Romano (2012). The fast fluidized bed carbonator model is briefly explained in the following while further details, including the manner in which it performs integration with a full process flowsheet, can be found in the relevant references (Romano, 2012; Ozcan et al., 2013). The model was developed with some assumptions such as uniform temperature; no interphase mass transfer resistance; perfect mixing of the solids; uniform particle size; and uniform superficial velocity. The model is based on the Kunii and Levenspiel (1991) CFB model operating in the fast fluidization regime. Two regions are distinguished inside the carbonator: a lower dense region and an upper lean region. A first order reaction is assumed for the carbonation reaction (Grasa et al., 2008). The model of Romano (2012) has provided satisfactory results when compared to experimental measurements obtained in lab-scale facilities at Stuttgart University, Germany and INCAR-CSIC, Spain (Charitos et al., 2011). The carbonator capture efficiency is strongly linked to the molar ratios of the fresh make-up sorbent-to-feed CO_2 (F_0/F_{CO_2}) and feed sorbent-to-feed CO_2 (F_R/F_{CO_2}). As a base study, the first ratio is fixed to 0.1 as this is the average value from different Ca-looping process simulation studies (Romano et al., 2012) while the latter is adjusted to reach an overall CO_2 capture efficiency of 90%. The overall CO_2 capture and CO_2 avoided efficiencies are calculated by the following equations.

$$\text{Overall } CO_2 \text{ capture efficiency} = \frac{\text{Amount of } CO_2 \text{ sent to storage}}{\text{Total amount of } CO_2 \text{ generated}} \quad (5)$$

$$CO_2 \text{ avoided efficiency} = \frac{CO_2 \text{ intensity}_{\text{reference plant}} - CO_2 \text{ intensity}_{\text{capture plant}}}{CO_2 \text{ intensity}_{\text{reference plant}}} \quad (6)$$

$$CO_2 \text{ intensity} = \frac{\text{Amount of } CO_2 \text{ emitted}}{\text{Net power capacity}} \quad (7)$$

where the "total amount of CO_2 generated" accounts for CO_2 created from fuel combustion and limestone calcination.

Five different cases have been examined by using the Ca–Cu looping and Ca-looping process simulations, and they are named Cases A to E. For both processes, Case A is the base case, for which the process specifications have already been given (0.1 F_0/F_{CO_2} and 90% overall CO_2 capture efficiency). In Case B, the CO_2 intensity reduces to 420 kg CO_2/MW_e that is the CO_2 capture target for coal-fired power plants in Canada (EC, 2013b). There is no cooling requirement in the carbonator of Case C since the entire excess heat in the carbonator can only satisfy the preheating requirement of the feed flue gas. The F_0/F_{CO_2} ratio which is a crucial carbonator input parameter is set to 0.05 and 0.15 in Cases D and E, respectively to investigate its effect on the net power efficiency.

The Ca–Cu sorbent that has been studied experimentally using a thermo-gravimetric analyser (TGA) is a physical mixture of Al_2O_3-stabilized CuO and Al_2O_3-stabilized CaO pellets. The compositions

of the two materials are 87 wt.% CuO/13 wt.% Al_2O_3 and 81 wt.% CaO/19 wt.% Al_2O_3. The CaO-based sorbent was synthesized using a sol-gel technique whereas the CuO-based CLC material was prepared using a co-precipitation approach. Details with regards to material synthesis can be found in Broda et al. (2012) and Imtiaz et al. (2012). In the TGA experiments, the sorbent was first calcined at 850 °C in 10% CH_4 (balance N_2) for 20 min. Subsequently the material was carbonated at 700 °C using 35 mol% CO_2 (balance N_2) for 40 min. The oxidation step took place at 950 °C in 10% O_2/90% N_2 for 25 min.

It should be noted that the experimental conditions do not exactly match the simulation conditions. For example, air is selected as the oxidation agent in the simulations, and the experimental cycle times are very long for the carbonator model used. Furthermore, because of the operational limitations of the TGA system, only 10% CH_4 was fed to the system instead of the 100% CH_4 assumed in the simulations. Nonetheless, we feel that the currently available experimental data and the implemented carbonator model are in fair agreement and are sufficient for a preliminary analysis of the proposed configuration. In addition, a sensitivity analysis on the sorbent performance is performed.

3.4. Heat exchanger network design for the Ca–Cu looping process

An important issue in the Ca–Cu looping systems is the recovery of heat from high temperature solid and gas streams as well as the exothermic carbonation reaction. It is, however, not possible to recover the thermal power used for limestone calcination unless the purge stream replaces partially the material feed of a cement plant. This option is not included in the scope of this work, and hence the energy required for calcination is lost. There are seven locations in the Ca–Cu looping process where the recovery of excess heat is needed (Fig. 2): the carbonator, the CO_2-depleted gas stream, the CO_2-rich gas stream, the solid stream from the air reactor to the carbonator, the purge stream, the O_2-depleted gas stream and the air reactor. While the latter is eliminated by the circulation of solids between the air reactor and the calciner, the excess heat from the high temperature O_2-depleted gas stream can be transferred to the air feed via a tubular regenerative air heater (DOE, 2003). A heat exchanger network (HEN) has been designed to recover the maximum excess heat for the generation of high temperature steam. The proposed HEN configuration is shown in Fig. 5 and has been supported by a pinch analysis for the estimation of minimum energy requirement (Linnhoff and Flower, 1978). The subcritical steam cycle configuration given for the reference power plant in Fig. 1 has been modified as an additional steam cycle for the recovery of excess heat provided in the Ca–Cu looping process. Hence, the boiler section in the reference steam cycle design is replaced with the available heat sources in the Ca–Cu looping process. Two important streams in the steam cycle for the production of high temperature steam are the boiler feedwater and cold reheat with temperatures of 252 °C and 366 °C, respectively. By considering a MTD of 20 °C, the CO_2-rich gas stream can be cooled to 272 °C while heating the boiler feedwater which is further heated by the transfer of excess heat in the carbonator and from the CO_2-depleted gas stream. Since the CO_2-rich stream is directly sent to the CO_2 compression unit rather than the stack, it can be further cooled through heat exchange with the methane feed entering the calciner. However, as a result of the very low heat duty required for preheating the methane feed stream, the amount of heat transfer between these streams is limited. Further heat transfer the CO_2-rich gas stream is only possible if part of the stream dilutions in the FWHs of the steam cycle can be replaced. Hence, the CO_2-rich gas stream can only be further cooled in two parallel feedwater heaters (PFWHs) as suggested in the DOE reports (DOE, 2003, 2010). The PFWHs are located between the streams 1–3 and 4–5 on the reference steam cycle given in Fig. 1. The temperatures of the streams 1, 3, 4 and 5 are 38.7 °C, 130.5 °C, 188.3 °C and 218.1 °C, respectively. The MTD in the PFWHs is also set to 20 °C. Furthermore, based on the temperature of the boiler feedwater after the second heat exchange step, the final temperature of the CO_2-depleted gas stream can be determined by respecting the MTD of 20 °C. This stream can then be further cooled to 135 °C by exchanging heat with the flue gas entering the carbonator. The main steam at 565 °C and 166.5 bar from the first part of the arrangement can then be sent to the HP turbine. In the second part of the arrangement, the reheat stream is heated to 565 °C and 38.3 bar by the transfer of excess heat from the purge stream and solid stream to the carbonator. The final temperature of the latter can be estimated when the temperature of the reheat stream after the first heat exchange step is known. Once this HEN arrangement is defined, the flow rate of the steam can be adjusted to minimize the energy requirement in the HEN.

The CO_2-rich gas stream leaving the PFWHs enters an induced fan to recover the pressure loss of 0.07 bar before being sent to the CO_2 compression (DOE, 2003). This assumption is also valid for the CO_2-rich gas streams from the Ca-looping and oxy-combustion processes detailed in the following sections. For the gas streams directly sent to the atmosphere, such as the CO_2-depleted gas stream, it is assumed that an induced fan compensates the pressure drop of 0.05 bar as for the flue gas from the reference power plant.

4. Reference power plant with the Ca-looping process

The schematic diagram of the Ca-looping process is presented in Fig. 6. The carbonator operates at 650 °C, and it is assumed that the CaO-based CO_2 sorbent is manufactured by the calcination of limestone that is assumed to be 100% $CaCO_3$. The following equation is used to describe the decrease in the maximum CaO conversion ($X_{max,N}$) of the sorbent after N cycles of carbonation/calcination (Li et al., 2008).

$$X_{\max,N} = a_1 f_1^{N+1} + a_2 f_2^{N+1} + b \tag{8}$$

where a_1, a_2, b, f_1, and f_2 are constants. According to the reports of Grasa and Abanades (2006) and Rodriguez et al. (2010), the values $a_1 = 0.1045$, $a_2 = 0.7786$, $b = 0.07709$, $f_1 = 0.9822$ and $f_2 = 0.7905$ represent well the behaviour of limestone and were, thus, used in Eq. (8) for the estimation of the $X_{max,N}$ in the carbonator model.

The calciner temperature is selected to be 900 °C, i.e. 15 °C in excess of the equilibrium temperature for the calcination reaction in a 100% CO_2 atmosphere (Garcia-Labiano et al., 2002). The heat requirement in the calciner is supplied by the combustion of fuel with oxygen from the ASU. The same type of coal that is fed to the boiler of the reference power plant is used in the calciner, and complete combustion of the coal is assumed. Since Genesee coal has very low sulphur content, the effect of sulphation on the CaO conversion of the sorbent was neglected. Nonetheless it is assumed that the SO_2 produced in the both combustors is fully captured by CaO due to the very high Ca/S ratios. It is also assumed that 80% of the ash from the coal combustion leaves the system as fly ash. The main concern of oxygen firing in the calciner is the difficulty to control the operating temperature. The potential problems include, but are not limited to, high flame temperatures and agglomeration concerns. Therefore, part of the CO_2-rich gas stream leaving the calciner is circulated and mixed with the oxygen feed to reduce the O_2 concentration and also to maintain the hydrodynamic conditions for fluidization. Up to 70 mol% oxygen firing in a bench scale fluidized bed combustion system has been successfully tested by the DOE (DOE, 2003). Hence, the O_2 concentration at the calciner inlet was set to 35 mol% in the simulated system. A fan is located on the circulated CO_2-rich gas stream to overcome the pressure drop of 0.2 bar

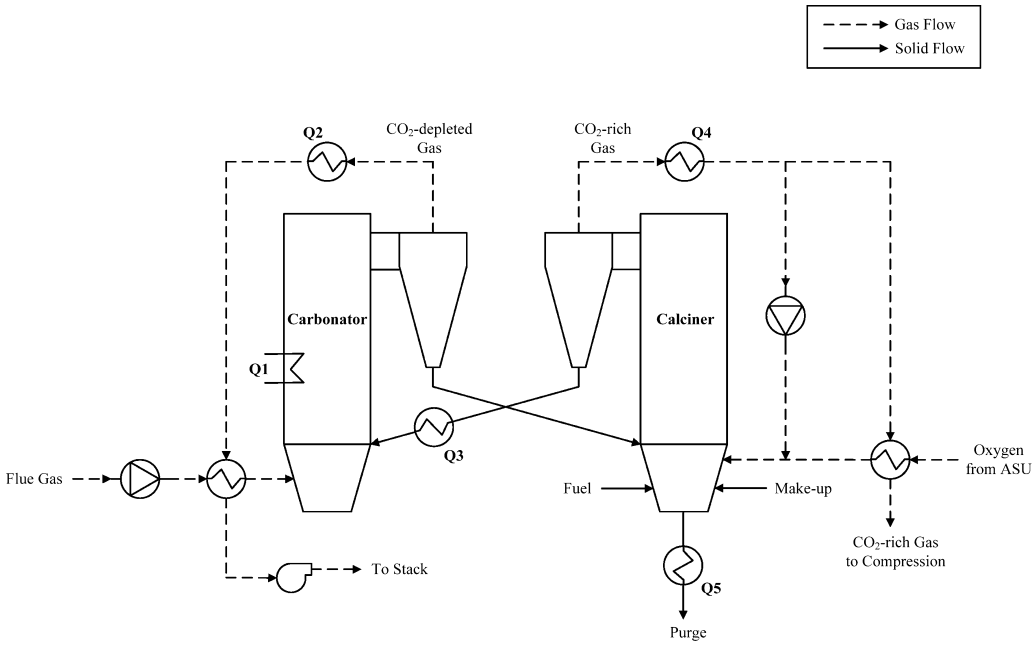

Fig. 6. Process diagram of the Ca-looping process.

in the calciner. It is assumed that the onsite ASU supplies oxygen at 1.2 bar with an energy requirement of 231 kWh/tonne O_2 (DOE, 2003). The purity of the oxygen feed is 99.1 mol%. The required oxygen flow rate is estimated by setting the molar fraction of O_2 in the CO_2-rich gas from the calciner to 3 mol% (wet-basis). The assumptions regarding sorbent attrition and infiltration air in the Ca-looping process are identical to those made for the Ca–Cu looping process. In terms of CO_2 purity, the Ca-looping system requires a purification stage in the CO_2 compression unit (Fig. 4b) to reach the minimum purity of ≥95 mol% CO_2.

There are five different locations in the Ca-looping process for heat recovery (see Fig. 6): the carbonator; the CO_2-depleted gas stream; solids from the calciner to carbonator; the CO_2-rich gas stream; and the purge stream. Since the streams and their temperatures are very similar to those in the Ca–Cu looping process, the HEN design proposed for the Ca–Cu looping process (Fig. 5) can also be implemented for the Ca-looping process. For further heat recovery from the CO_2-rich gas stream, a PFWH is added between streams 1 and 3 in the steam cycle presented in Fig. 1 to satisfy partially the heat requirement in the FWHs 1–4.

5. Oxy-firing power plant

The oxy-firing CFB power plant has the same thermal input as the reference power plant but contains two additional units: a cryogenic ASU for oxygen production and a CO_2 CPU. The main difference of the oxy-firing CFB plant compared to the air-fired system presented in Fig. 1 is the replacement of the combustion air with high purity oxygen. Therefore, not only the CO_2 concentration in the flue gas increases but also the heat requirement for nitrogen preheating is avoided. The assumptions made for the calciner of Ca-looping process such as combustion efficiency and molar fraction of O_2 in the feed gas have been also adopted for the oxy-firing combustor since their operating conditions are very similar. Also, the assumptions of limestone injection and air infiltration are kept similar to those in the reference power plant. The CO_2-rich gas stream from the convection pass heat exchangers is further cooled to 80 °C in a PFWH located between streams 1 and 2 (at 115.6 °C) in the steam cycle presented in Fig. 1. For the oxy-firing power plant, the CO_2 capture efficiency would be equal to almost 100% if the CO_2 purification stage is not required. However, the capture efficiency reduces along with the separation efficiency of the purification stage.

6. Reference power plant with the amine scrubbing process

Finally, a conventional MEA-based capture process is integrated into the reference power plant. The schematic diagram of the amine scrubbing process for CO_2 capture is shown in Fig. 7. This system comprises an absorber for CO_2 capture and a desorber for the regeneration of the solvent. To obtain accurate performance predictions in these units, the add-on amine thermodynamic package in UniSim Design is used. The technical modelling parameters and the design procedure for the amine-based capture process detailed in Ahn et al. (2013) and DOE (2007) are adapted here.

The level of the NO_x and SO_x concentrations in the flue gas stream is crucial for the MEA process. These components react with amine to produce amine salts which cannot be dissociated in the stripper. To make the CO_2 absorption using MEA economic, the SO_2 and NO_2 concentrations in the flue gas stream should be restricted to approximately 10 ppm and 20 ppm, respectively (IEA, 2008). Following the suggestions of the IEAGHG (2009), an external selective catalytic reduction unit is not included because of the very low NO_x emissions and the possibility to inject ammonia in the furnace. However, the SO_2 emission limits cannot be achieved by only limestone injection into the boiler of the reference power plant; therefore an external flue gas desulphurization unit (FGD) is included. The flue gas stream enters the FGD unit at 135 °C and it is subsequently sent to a cooler, where it is cooled to 32 °C and part of the water in this stream is condensed out. The stream is then pressurized to 1.31 bar by a blower prior to the absorption stage. The lean amine concentration is set to 30 wt% by adjusting the MEA and water make-up flowrates. The CO_2-rich sorbent is pumped to the striper which operates at 1.93 bar at the bottom. A water wash tower is included for the recovery of vaporized MEA which is then sent back to the absorber.

An important design issue for the amine scrubbing process is to satisfy heat duty in the steam stripper for solvent regeneration. According to the relevant references (DOE, 2007; Ahn et al., 2013), it is preferable to extract the steam from the IP/LP crossover (stream

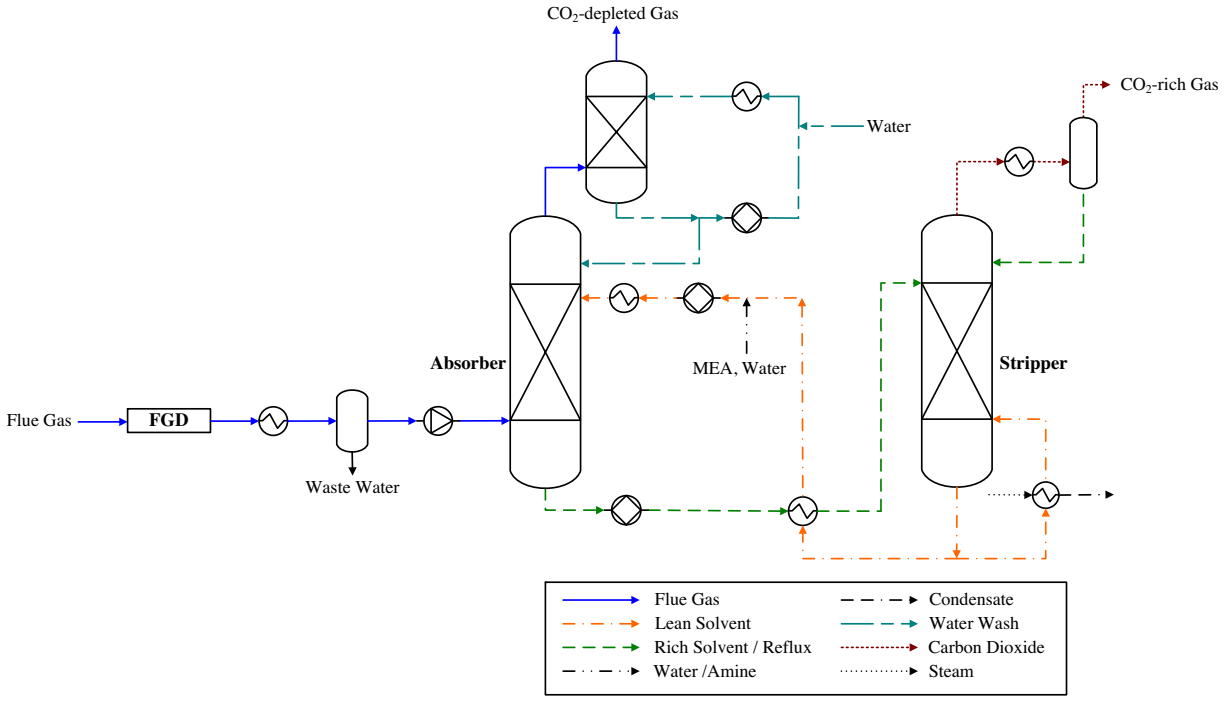

Fig. 7. The schematic diagram of the conventional MEA-based CO_2 capture process integrated to the reference power plant presented in Fig. 1. FGD: Flue gas desulphurization unit, MEA: monoethanolamine.

6 in Fig. 1) in the steam cycle that is expanded from 11.6 bar to 3.1 bar by a let-down turbine. The superheated steam can be further cooled to a saturated steam with a temperature of 134 °C in a desuperheater and is transferred to the stripper with a reboiler temperature of 120 °C. After the use of steam extraction, the condensed water from the reboiler is pumped to 11.7 bar and is returned to the deaerator. The purity of the CO_2-rich gas stream from the stripper is already very high (~96 mol%) such that the basic CO_2 compression unit configuration given in Fig. 4a is employed in the amine scrubbing process.

7. Results and discussion

7.1. Reference power plant

Burning 103.45 tonne/h coal with a LHV of 21.67 MJ/kg in the boiler of the reference power plant, the total thermal power input from coal combustion is estimated to be 622.7 MW_{th}, which is converted to 269.9 MW_e power with a gross power efficiency of 43.3%. The power requirements of the plant auxiliaries are calculated to be 19.9 MW_e, which results the net power generation capacity of 250 MW_e with a net power efficiency of 40.1%. Furthermore, the CO_2 intensity of the reference power plant is calculated to be 825.2 kg CO_2/MW_e.

7.2. Reference power plant with the Ca–Cu looping/Ca-looping processes

The experimental performances of the Ca–Cu sorbent with an overall composition of 74.0 wt.% CaO, 7.5 wt.% CuO and 18.5 wt.% Al_2O_3 are presented in Fig. 8. In addition, the cyclic CO_2 uptake of limestone (Grasa and Abanades, 2006) is given for comparison. Using mass and energy balance calculations with experimental data given in Fig. 8, the overall composition of the Ca–Cu sorbent was estimated by the process simulator as 76.3 wt.% CaO, 5.0 wt.% CuO and 18.7 wt.% Al_2O_3. This composition is very close to the composition of the experimentally assessed material. The CaO conversion of the Ca–Cu sorbent is higher in the first 60 cycles but reduces the same values of limestone afterwards. The experimental CaO conversion curve of the Ca–Cu sorbent was fitted by Eq. (8), and the conversion data was used in the carbonator model. The fitting constants obtained are summarized in Table 4. The experimental data was fitted by two curves to increase the accuracy. The first set of parameters fits the experimental data for cycle numbers ≤19 and the second set for the remaining cycles (up to 24 cycles). After a rapid increase in CuO conversion of the Ca–Cu sorbent in the first 4 cycles, the CuO conversion remains stable until the 24th cycle. This behaviour supports the idea of recycling purged CuO in the capture system (Qin et al., 2012; Kierzkowska and Müller, 2013).

The pinch analysis specifications for Case A of the Ca–Cu looping process (Table 5) and that of the Ca-looping process (Table 6) include the supply and target temperatures, heat duty and stream type (hot or cold) of each stream defined in the HEN. The minimum energy requirements for these systems that are calculated by pinch analysis are equal to zero when the flow rates of steam in the additional steam cycles are set to 388.3 tonne/h and 580.5 tonne/h for the Ca–Cu looping and the Ca-looping processes, respectively. Thus, this represents the maximum heat recovery from these processes. The grand composite curves (GCCs) for these systems, developed by using the pinch analysis and presented in Fig. 9, prove the minimization of cold and hot utilities in the proposed HEN.

The process performances of Cases A to E for the Ca–Cu looping and Ca-looping processes are given in Tables 7 and 8, respectively. For each Ca-looping simulation case, results for both coal-fired and methane-fired calciners are presented. Unless values are the same, those presented in parentheses refer to methane combustion in the calciner and allow a more appropriate comparison between the Ca-looping and the Ca–Cu looping processes. In the case of methane combustion, a larger quantity of H_2O is generated such that the calciner of Ca-looping process can operate at 880 °C to achieve full calcination of the sorbent. The total thermal power input, when

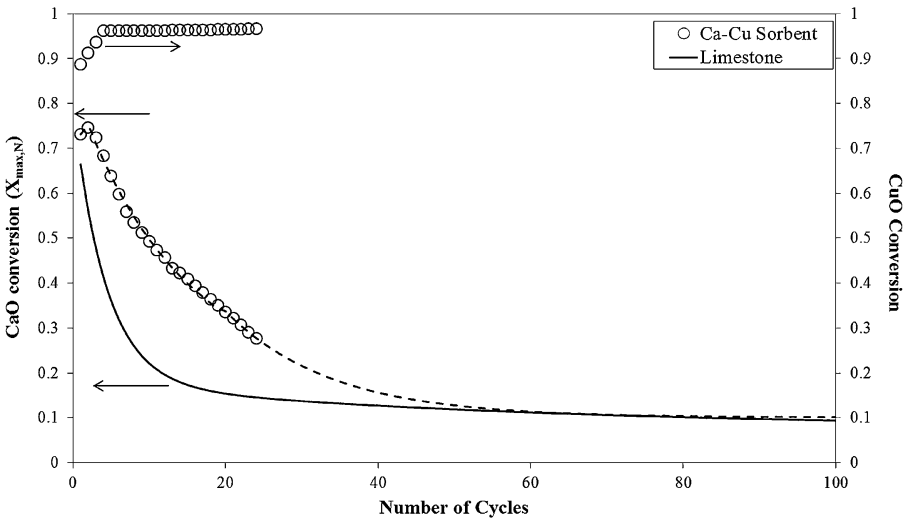

Fig. 8. Experimental CaO and CuO cyclic conversions of the Ca–Cu sorbent (74 wt.% CaO/7.5 wt.% CuO/Al_2O_3) and CaO conversion of limestone (Grasa and Abanades, 2006). The dashed line is generated using the fitting parameters given in Table 4.

Table 4
The fitting parameters for the CaO conversion of the Ca–Cu sorbent.

	a_1	a_2	f_1	f_2	b
($N \leq 19$)	−25.94	0.7126	0.04966	0.929	0.1801
($N > 19$)	1.072	2.968	0.9306	0.3252	0.1006

either the Ca–Cu looping or the Ca-looping process is added, is the summation of the thermal power supplied to the reference power plant (622.7 MW_{th}) and that of the capture process. The total thermal power requirements in the Ca–Cu looping cases are less than those estimated for the Ca-looping process. This is because of the higher average CaO conversion (X_{ave}) of the Ca–Cu sorbent and the corresponding reduction in the sorbent circulation between the reactors (F_R/F_{CO_2}). The total thermal power inputs in the Ca-looping cases reach almost double of that of the reference power plant. The required F_R/F_{CO_2} ratios were estimated to ensure an overall CO_2 capture efficiency of 90% in Cases A, D and E. A reduction in F_0/F_{CO_2} in Case D of both processes requires greater F_R/F_{CO_2} ratios because of the reduction in X_{ave} of the sorbents. In contrast, by increasing the addition of fresh sorbent (Case E), X_{ave} of the sorbents can be increased, and the required F_R/F_{CO_2} ratios decrease. For the Ca-looping cases, the F_R/F_{CO_2} estimates where methane is used as a fuel in the calciner are slightly higher than for the use of coal. This is due to the fact that the specific CO_2 emissions (kg CO_2/MW_{th}) from coal combustion are greater compared to those of methane combustion. Therefore, more CO_2 should be captured in the carbonator coupled with a methane-fired calciner in the Ca-looping process to achieve the same overall CO_2 capture efficiency as a coal-fired calciner.

The gross power capacity estimates given in Tables 7 and 8 for the different cases are the summation of that of the reference power plant and the capture process. The value of the first was calculated to be 276 MW_e considering additional heat recovery from the flue gas stream before the carbonator. The maximum gross power capacity reaches 544.5 MW_e in Case D of the Ca-looping process owing to a very high F_R/F_{CO_2} that corresponds to a high thermal power requirement. When the gross power efficiency estimates for the Ca–Cu looping and the Ca-looping processes are compared, it can be observed that those for the Ca-looping process are higher. This is due to the fact that the fraction of heat loss from the calcination of the make-up limestone reduces with increasing total thermal power input. For the same reason, although the heat consumption for the make-up limestone calcination is exactly the same among Cases A to C in both capture processes, the gross power efficiencies in Cases A are greater. The highest gross power efficiencies are achieved in Cases D due to the smaller quantity of heat required for calcination.

The power requirement in the ASU is proportional to the thermal power requirement in the Ca-looping process whereas the power requirement in the CO_2 CPU corresponds to the amount of CO_2 captured. While the power requirement for the ASU is around 0.065 MW_e per each MW_{th} supplied to the calciner by coal combustion, this value increases to around 0.072 MW_e/MW_{th} when methane is used as a fuel in the calciner. Considering the power requirements of the plant auxiliaries (both for the reference power plant and the Ca-looping process), ASU and CO_2 CPU, the new net power generation capacity of the Ca-looping system can reach up to 400.9 MW_e depending on the overall CO_2 capture efficiency, the calciner fuel and the F_0/F_{CO_2} ratio. The net power efficiency of the Ca-looping process is the lowest for Case E (31.4% for methane combustion) owing to the great heat loss linked to the calcination of the make-up sorbent, but increases up to 32.9% in Case D at the same overall CO_2 capture efficiency. The energy penalty of CO_2 capture by the Ca-looping process using a coal-fired calciner ranges from 7.8 percentage points to 9.2 percentage points at 90% overall CO_2 capture efficiency according to the results presented in Table 8. These energy penalty estimates are in a fair agreement with those reported in Romano et al. (2012) for different Ca-looping studies. While the overall CO_2 capture efficiency decreases to around 45% in Case C of the Ca-looping process, the CO_2 avoided efficiency is as high as 89.8% in Case D depending on the CO_2 intensity of this system.

Most importantly, the net power efficiency values for the Ca–Cu looping process are higher than those estimated for the Ca-looping process mainly as a result of the absence of the ASU. In addition, the power requirement in the CO_2 compression unit reduces as no CO_2 purification stage is needed in the Ca–Cu looping process. Without the CO_2 purification stage, the approximate composition of the liquid CO_2 stream from the Ca–Cu looping process is as follows (mol%): 96.2% CO_2, 2.8% N_2, 0.8% O_2 and 0.2% H_2O and that of the Ca-looping process after the purification stage is as follows (mol%): 96.7% CO_2, 1.4% N_2, 1.6% O_2 and 0.3% H_2O. For both processes, the O_2 content of the final gas is within the recommended limits for enhanced oil recovery and saline reservoir sequestration (DOE, 2012). When lowering the make-up flow, the net power efficiency reaches 36.6% with a CO_2 avoided efficiency of 90.4% in Case D of the Ca–Cu looping process. A greater improvement in the net power efficiency is possible when the make-up flow is further reduced in both capture

Table 5
Pinch analysis specifications for the Ca–Cu looping process (Case A).

Heat recovery location	Supply temperature (°C)	Target temperature (°C)	Heat duty (MW_{th})	Stream type
Carbonator	650.0	650.0	116.6	Hot
CO_2-depleted Gas	650.0	135.0	120.2	Hot
CO_2-rich Gas (from calciner)	885.0	272.0	76.2	Hot
CO_2-rich Gas (to compression)	267.0[a]	80.0	20.2	Hot
Solids from air reactor to carbonator	950.0	758.0	41.4	Hot
Purge from air reactor	950.0	386.0	5.3	Hot
Flue gas to carbonator	115.0[b]	320.0	56.2	Cold
Cold reheat	366.0	565.6	46.7	Cold
Boiler feedwater	252.0	565.6	256.8	Cold
Feedwater (str. 1–3 in Fig. 1)	38.7	130.5	13.3	Cold
Feedwater (str. 4–5 in Fig. 1)	180.3	218.1	6.9	Cold

[a] The reduction in the temperature is related to the flow of infiltration air into the convection pass heat exchangers.
[b] It is the temperature of flue gas stream after the fan.

Table 6
Pinch analysis specifications for the Ca-looping process (Case A).

Heat Recovery Location	Supply temperature (°C)	Target temperature (°C)	Heat duty (MW_{th})	Stream type
Carbonator	650.0	650.0	152.8	Hot
CO_2-depleted gas	650.0	135.0	119.5	Hot
Solids from calciner to carbonator	900.0	764.0	65.6	Hot
CO_2-rich gas (from calciner)	900.0	272.0	167.4	Hot
CO_2-rich gas (to compression)	267.4[a]	80.0	23.0	Hot
Purge from calciner	900.0	386.0	4.2	Hot
Oxygen feed to calciner	15.0	247.0	8.6	Cold
Flue gas to carbonator	115.0[b]	319.0	55.9	Cold
Cold reheat	366.0	565.6	69.8	Cold
Boiler feedwater	252.0	565.6	383.8	Cold
Feedwater (str. 1–3 in Fig. 1)	38.7	130.5	14.4	Cold

[a] The reduction in the temperature is related to the flow of infiltration air into the convection pass heat exchangers.
[b] It is the temperature of flue gas stream after the fan.

processes. However, this results in a further increase in the flow of sorbent between the reactors (F_R/F_{CO_2}) because of the decay in X_{ave} of the sorbents.

The sensitivity of the results for the Ca–Cu looping process against the CaO conversion of the Ca–Cu sorbent is given in Fig. 10. Although it is not possible to predict precisely the CaO conversion behaviour of a sorbent without conducting the relevant experiments, the CaO conversion of the Ca–Cu sorbent presented in Fig. 8 has been reduced by 25% and 50% relative to Case A. The ratio of F_0/F_{CO_2} has been retained at 0.1. Therefore, the main difference results from the change in the F_R/F_{CO_2} required to achieve an overall CO_2 capture efficiency of 90%. By lowering the sorbent

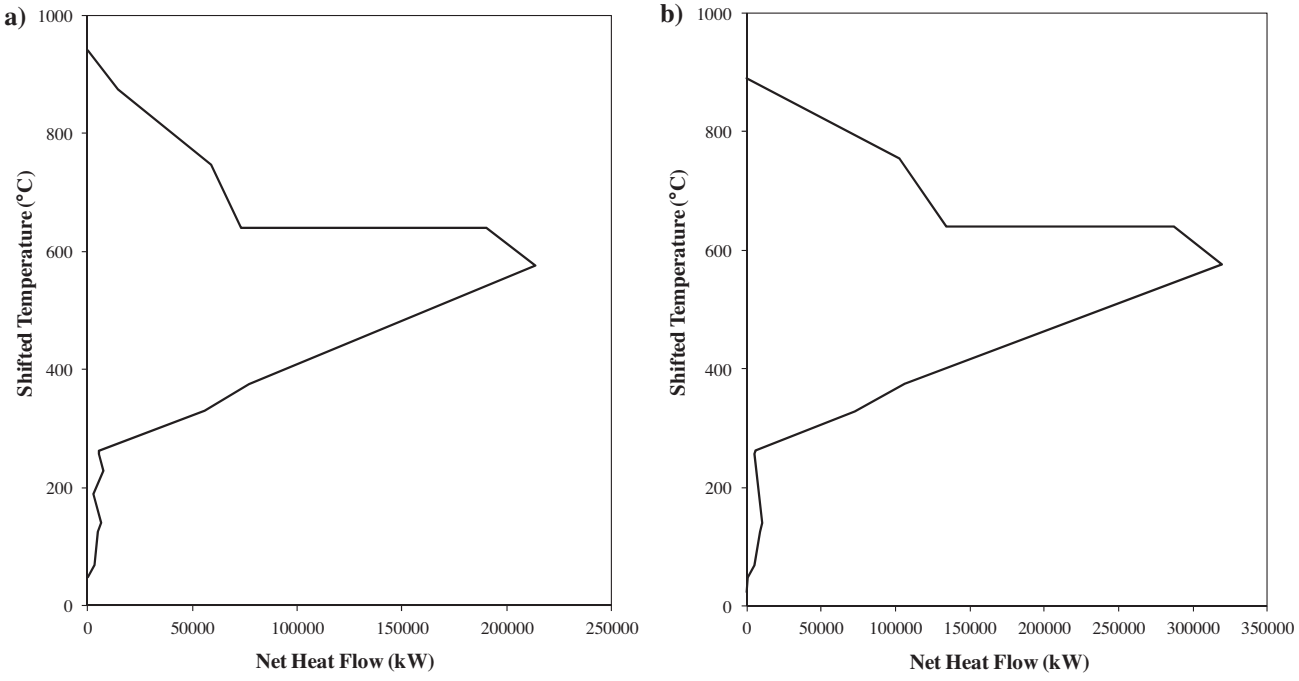

Fig. 9. Grand composite curves (GCCs) developed by using the pinch analysis specifications given in: (a) Table 5 for the Ca–Cu looping process (Case A); and (b) Table 6 for the Ca-looping process (Case A).

Table 7
The process performance of the Ca–Cu looping process at different cases.

	Case A	Case B	Case C	Case D	Case E
Total thermal power input (MW_{th})	985.0	808.4	780.9	1026.1	990.0
F_0/F_{CO_2}	0.1	0.1	0.1	0.05	0.15
F_R/F_{CO_2}	2.2	0.7	0.5	4.1	1.7
X_{ave}	0.39	0.58	0.66	0.21	0.5
Gross power capacity (MW_e)/efficiency (%)	419.7/42.6	341.8/42.3	329.8/42.2	445.1/43.4	415.1/41.9
Plant auxiliaries (MW_e)	19.9 + 20.6	19.9 + 14.9	19.9 + 13.9	19.9 + 21.5	19.9 + 21.1
CO_2 compression unit power (MW_e)	28.7	15.2	12.9	28.4	29.9
Net power capacity (MW_e)/efficiency (%)	350.5/35.6	291.8/36.1	283.1/36.3	375.3/36.6	344.2/34.8
CO_2 capture efficiency in the carbonator (%)	85.4	40.6	32.9	85.6	84.8
Overall CO_2 capture efficiency (%)	90.0	53.9	46.9	90.0	90.0
CO_2 intensity (kg CO_2/MW_e)	85.9	420.0	488.8	79.5	91.2
CO_2 avoided efficiency (%)	89.6	49.1	40.8	90.4	89.0

performance by 25% and 50%, the required F_R/F_{CO_2} increases to 3.8 and 8.5, respectively. The latter is greater than that of Case A in the Ca-looping process and illustrates when the performance of the Ca–Cu sorbent is worse than that of the limestone in the Ca-looping case. At very high F_R/F_{CO_2} ratios, the solid circulation rate between the reactors increases and this enhances the thermal power requirement in the system. With a reduction of 50% in the sorbent performance, the total thermal power requirement increases by 21%. As mentioned before, such changes in the thermal power input lead to an increase in the gross power capacity of the plant because the heat loss from the make-up calcination becomes less effective. The net power efficiency also increases for the same reason and slightly improves the CO_2 avoided efficiency. However, it should be emphasized again that significantly high solid circulation rates can potentially create difficulties in operation. Importantly, the sensitivity analysis illustrates the superiority of the energy performance of the Ca–Cu looping process against that of the Ca-looping even with a less efficient sorbent. In conclusion, it is clear that the Ca–Cu looping process is an effective way of reducing the energy penalty of the Ca-looping process. Comparing Cases A using methane as fuel in both systems, it can be observed that the improvement is around 3.4 percentage points. However, a detailed cost analysis of the Ca–Cu material is required to reveal the full process economics and have a more appropriate comparison with the Ca-looping process.

7.3. Oxy-firing power plant

Although the thermal power input in the reference and oxy-firing power plants are identical, viz. 622.7 MW_{th}, the gross power generation capacity of the latter is slightly higher, i.e. 280.3 MW_e, giving a gross power efficiency of 45.0%. As mentioned, this difference is due to the absence of the preheating requirement for nitrogen and a greater heat recovery from the CO_2-rich gas stream leaving the boiler. However, additional power requirements of 39.1 MW_e for the ASU, 27.0 MW_e for the CO_2 CPU and 18.5 MW_e for the plant auxiliaries reduce the net power generation capacity to 195.7 MW_e corresponding to a net power efficiency of 31.4% and an energy penalty of 8.7 percentage points. The energy penalty estimated for the oxy-firing power plant in this study is in the range of those reported in Dickmeis and Kather (2014) (~8.3 percentage points) and IEAGHG (2014) (~9 percentage points). The overall CO_2 capture efficiency of the oxy-firing power plant is 94.3%, which is the separation efficiency in the CO_2 purification stage. The final gas composition after the CO_2 CPU is very similar to that given for the Ca-looping process as both systems use oxy-firing combustors. The CO_2 intensity of the oxy-firing power plant is 60.6 kg CO_2/MW_e corresponding to a CO_2 avoided efficiency of 92.7%. In terms of net power efficiency, the oxy-firing power plant is competitive with the Ca-looping process. Although the gross power efficiency of the first is greater because of the heat loss associated with the calcination of the make-up sorbent stream in the Ca-looping process, the gain from the use of less oxygen in the calciner improves the net power efficiency of the Ca-looping process. The difference in the net power efficiency increases further by reducing the make-up flow (as in Case D) whereas further heat loss from make-up calcination makes the oxy-combustion process favourable. All net power capacity estimates for the Ca–Cu looping and Ca-looping processes studied are greater than 250 MW_e, i.e. the net output of the reference power plant. An additional source of power would be required for the oxy-firing power plant to obtain the net power

Table 8
The process performance of the Ca-looping process at different cases.

	Case A	Case B	Case C	Case D	Case E
Total thermal power input (MW_{th})	1127.3 (1111.2)	865.5 (857.0)	805.0 (804.1)	1241.5 (1149.3)	1105.6 (1103.4)
F_0/F_{CO_2}	0.1	0.1	0.1	0.05	0.15
F_R/F_{CO_2}	5.6 (6.2)	1.7	1.0 (1.1)	8.3 (9.0)	4.3 (4.7)
X_{ave}	0.16 (0.15)	0.26	0.32 (0.29)	0.11 (0.10)	0.20 (0.19)
Gross power capacity (MW_e)	486.2 (480.4)	368.8 (365.8)	341.7 (341.8)	544.5 (504.5)	469.7 (470.1)
Gross power efficiency (%)	43.1 (43.2)	42.6 (42.7)	42.4 (42.5)	43.9 (43.9)	42.5 (42.6)
Plant auxiliaries (MW_e)	43.4 (43.0)	35.7 (35.5)	34.0 (34.0)	46.4 (43.8)	43.1 (43.1)
ASU power (MW_e)	32.8 (35.0)	15.8 (16.8)	11.9 (13.1)	39.9 (37.6)	31.4 (34.5)
CO_2 CPU (MW_e)	53.5 (44.9)	28.5 (23.7)	21.3 (18.2)	57.3 (44.6)	53.9 (46.2)
Net power capacity (MW_e)	356.5 (357.5)	288.8 (289.8)	274.5 (276.5)	400.9 (378.5)	341.3 (346.3)
Net power efficiency (%)	31.6 (32.2)	33.4 (33.8)	34.1 (34.4)	32.3 (32.9)	30.9 (31.4)
CO_2 capture efficiency in the carbonator (%)	87.8 (91.9)	44.1	31.6 (32.4)	87.5(92.4)	87.5 (91.4)
Overall CO_2 capture efficiency (%)	90.0	60.7 (55.9)	49.3 (45.1)	90.0	90.0
CO_2 intensity (kg CO_2/MW_e)	110.8 (90.7)	420.0	534.0 (526.2)	105.3 (84.6)	117.3 (96.3)
CO_2 avoided efficiency (%)	86.6 (89.0)	49.1	35.3 (36.2)	87.2 (89.8)	85.8 (88.3)

The results given in the parenthesis are based on a methane-fired calciner.

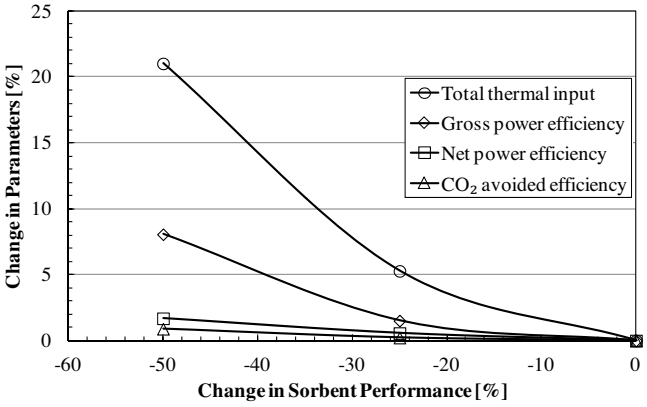

Fig. 10. The sensitivities of total thermal input, gross and net power efficiencies, and CO_2 avoided efficiency estimates against the change in the CaO conversion of the Ca–Cu sorbent presented in Fig. 8 relative to Case A in the Ca–Cu looping process.

output of the reference power plant. On the other hand, we would like to highlight that the CO_2 avoided efficiency is higher in the oxy-firing power plant and is only limited to the separation efficiency in the purification stage whereas achieving such high efficiencies are challenging for the Ca–Cu looping and Ca-looping processes due to equilibrium limitations for the carbonation/calcination reactions.

7.4. Reference power plant with the amine scrubbing process

For the amine scrubbing configuration, the total thermal power requirement is also equal to that of the reference power plant. The extraction of steam from the IP/LP crossover reduces the gross power generation capacity to 226.6 MW_e when the overall CO_2 avoided efficiency is 90%. The thermal energy consumption in the stripper boiler is estimated to be 3.55 $MJ_{th}/kg\,CO_2$ which is in agreement with the experimental and simulation studies, e.g. Alie et al. (2005) and Tobiesen et al. (2008). The additional power consumptions for the reference power plant auxiliaries (19.6 MW_e), amine plant auxiliaries (7.0 MW_e), and CO_2 compression unit (15.4 MW_e) reduce the net power generation capacity to 184.6 MW_e, which represents a net power efficiency of 29.6%. Although the power requirement of the CO_2 compression unit in the amine scrubbing process is less than those estimated in the oxy-firing power plant and the Ca-looping process, the net power efficiency of this system is the lowest among the capture processes studied here. The results justify the need of more advanced CO_2 capture technologies for the reduction of energy penalties associated with CO_2 capture.

8. Conclusions

The process design of a Ca–Cu looping process where the heat requirement in the calciner is met by the reduction of CuO with methane has been carried out. This CO_2 capture architecture has been integrated into a 250 MW_e power plant with a net power efficiency of 40.1%, and the variation in total energy consumption has been determined. In addition, the technical performances of alternative technologies such as oxy-combustion, Ca-looping and amine scrubbing have been evaluated for comparison. The Ca–Cu looping process eliminates the need of an energy intensive ASU. Here, the configuration using a solid circulation route of carbonator → calciner → air reactor → carbonator has been selected to allow the transfer of heat between the air reactor and calciner by hot solid circulation. The net power efficiency of this process with an overall CO_2 capture efficiency of 90% increases up to 36.6% at 0.05 F_0/F_{CO_2}. However, further studies are still required to investigate the economic performance of this process since the cost of the sorbent could be comparatively high, unless CuO/Al_2O_3 pellets can be separated from the purge and fly ashes and reused in the system. Furthermore, the results obtained here are based on predictions and represent high-end values. Further validation of the process is still needed. On the other hand, the net power efficiency of the Ca-looping process is as high as 32.9% (at 0.05 F_0/F_{CO_2}) at an overall CO_2 capture efficiency of 90%. Further improvements in the net efficiencies of the Ca–Cu looping and Ca-looping processes are possible if the purge flow rate can be decreased. However, this will in turn increase the total thermal power requirements of these systems and complicate the solid circulation between the reactors. The net power efficiency decreases to 31.4% in the oxy-firing plant mainly because of the power requirements for the ASU and CO_2 CPU. Here, an overall CO_2 capture efficiency of 94.3% is achieved. Although the amine scrubbing process is closest to commercialization, this technology comes with the highest energy penalty (10.5 percentage points) among the CO_2 capture technologies studied here. Moreover, it is found that a power plant integrated with either an amine scrubbing process or an oxy-combustion process suffers from the reduction in the net power capacity. On the other hand, if CO_2 capture is realized via either the Ca–Cu looping process or the Ca-looping process, the net power capacity increases.

Acknowledgements

The authors acknowledge financial support from the Turkish Ministry of Education and the joint travel fund from UKCCS Research Centre and Carbon Management Canada (CMC).

References

Abanades, J.C., Murillo, R., 2009. Method of Capturing CO_2 by Means of CaO and the Exothermal Reduction of a Solid. European Patent Application EP2305366 A1.
Abanades, J.C., Murillo, R., Fernandez, J.R., Grasa, G., Martinez, I., 2010. New CO_2 capture process for hydrogen production combining Ca and Cu chemical loops. Environ. Sci. Technol. 44, 6901–6904.
Ahn, H., Luberti, M., Liu, Z., Brandani, S., 2013. Process configuration studies of the amine capture process for coal-fired power plants. Int. J. Greenh. Gas Control 16, 29–40.
Alie, C., Backham, L., Croiset, E., Douglas, P.L., 2005. Simulation of CO_2 capture using MEA scrubbing: a flowsheet decomposition method. Energy Convers. Manage. 46 (3), 475–487.
Arias, B., Diego, M.E., Abanades, J.C., Lorenzo, M., Diaz, L., Martinez, D., Alvarez, J., Sanchez-Biezma, A., 2013. Demonstration of steady state CO_2 capture in a 1.7 MW_{th} calcium looping pilot. Int. J. Greenh. Gas Control 18, 237–245.
Bandyopadhyay, A., 2011. Amine versus ammonia absorption of CO_2 as a measure of reducing GHG emission: a critical analysis. Clean Technol. Environ. Policy 13 (2), 269–294.
Broda, M., Kierzkowska, A.M., Müller, C.R., 2012. Application of the sol–gel technique to develop synthetic calcium-based sorbents with excellent carbon dioxide capture characteristics. ChemSusChem 5 (2), 411–418.
Caldecott, B., Dericks, G., Mitchell, J., 2015. Stranded Assets and Subcritical Coal: The Risk to Companies and Investors. Smith School Enterprise and the Environmental, Oxford University, Retrieved from http://www.smithschool.ox.ac.uk/research-programmes/stranded-assets/Stranded%20Assets%20and%20Subcritcial%20Coal%20-%20The%20Risk%20to%20Investors%20and%20Companies%20-%20April15.pdf.
Chang, M.H., Huang, C.M., Liu, W.H., Chen, W.C., Cheng, J.Y., Chen, W., Hsu, H.W., 2013. Design and experimental investigation of calcium looping process for 3-kW_{th} and 1.9-MW_{th} facilities. Chem. Eng. Technol. 36 (9), 1525–1532.
Charitos, A., Rodriguez, N., Hawthorne, C., Alonso, M., Zieba, M., Arias, B., Kopanakis, G., Scheffknecht, G., Abanades, J.C., 2011. Experimental validation of the calcium looping CO_2 capture process with two circulating fluidized bed carbonator reactors. Ind. Eng. Chem. Res. 50, 9685–9695.
Curran, G.P., Fink, C.E., Gorin, E., 1967. Carbon dioxide-acceptor gasification process: studies of acceptor properties. Adv. Chem. Serv. 69, 141–165.
de Diego, L.F., Garcíía-Labiano, F., Adánez, J., Gayán, P., Abad, A., Corbella, B.M., Maríía Palacios, J., 2004. Development of Cu-based oxygen carriers for chemical-looping combustion. Fuel 83 (13), 1749–1757.
Dean, C.C., Dugwell, D., Fennell, P.S., 2011a. Investigation into potential synergy between power generation, cement manufacture and CO_2 abatement using the calcium looping cycle. Energy Environ. Sci. 4 (6), 2050–2053.
Dean, C.C., Blamey, J., Florin, N.H., Al-Jeboori, M.J., Fennell, P.S., 2011b. The calcium looping cycle for CO_2 capture from power generation, cement manufacture and hydrogen production. Chem. Eng. Res. Des. 89 (6), 836–855.

Dickmeis, J., Kather, A., 2014. The coal-fired oxyfuel-process with additional gas treatment of the ventgas for increased capture rates. Energy Procedia 63, 332–341.
Dlugokencky, E., Tans, P., 2014. NOAA/ESRL, http://www.esrl.noaa.gov/gmd/ccgg/trends/.
DOE, 1999. Carbon Sequestration: Research and Development. U.S. Department of Energy Report, Office of Science, Office of Fossil Energy, U.S. Department of Energy.
DOE, 2003. Greenhouse Gas Emissions Control by Oxygen Firing in Circulating Fluidized Bed Boilers: Phase 1 – A Preliminary Systems Evaluation. Prepared by Marion, J.L., Bozzuto, C.R., Nsakala, N.Y., Liljedahl, G.N., Andrus, H.E., Chamberland, R.P. Alstom Power Inc. and National Energy Technology Laboratory.
DOE, 2007. Cost and Performance Baseline for Fossil Energy Plants. Volume 1: Bituminous Coal and Natural Gas to Electricity Final Report 2007, NETL-2007/1281.
DOE, 2010. Cost and Performance for Low-Rank Pulverized Coal Oxycombustion Energy Plants, Final Report 2010, NETL-401/093010.
DOE, 2012. Quality Guidelines for Energy System Studies: CO_2 Impurity Design Parameters, DOE/NETL-341/011212.
EC, 2013a. Canada's Emission Trends. Environment Canada, ISSN 2291-9392.
EC, 2013b. Coal-Fired Electricity Generation Regulations – Overview. Environment Canada, Retrieved from: https://www.ec.gc.ca/cc/default.asp?lang=En&n=C94FABDA-1 (31.01.15).
EPRI, 2009. Updated Cost and Performance Estimates for Clean Coal Technologies Including CO_2 Capture – 2009. Electric Power Research Institute, Palo Alto, CA.
Fennell, P.S., Davidson, J.F., Dennis, J.S., Hayhurst, A.N., 2007. Regeneration of sintered limestone sorbents for the sequestration of CO_2, from combustion and other systems. J. Energy Inst. 80, 116–119.
Fernandez, J.R., Abanades, J.C., Murillo, R., Grasa, G., 2012. Conceptual design of a hydrogen production process from natural gas with CO_2 capture using a Ca–Cu chemical loop. Int. J. Greenh. Gas Control 6, 126–141.
Forero, C.R., Gayán, P., García-Labiano, F., De Diego, L.F., Abad, A., Adánez, J., 2011. High temperature behaviour of a $CuO/\gamma Al_2O_3$ oxygen carrier for chemical-looping combustion. Int. J. Greenh. Gas Control 5 (4), 659–667.
Finkenrath, M., (No. 2011/5) 2011. Cost and Performance of Carbon Dioxide Capture from Power Generation. OECD Publishing.
Garcia-Labiano, F., Abad, A., de Diego, L.F., Gayan, P., Adanez, J., 2002. Calcination of calcium-based sorbents at pressure in a broad range of CO_2 concentrations. Chem. Eng. Sci. 57, 2381–2393.
Garcia-Labiano, F., De Diego, L.F., Adánez, J., Abad, A., Gayán, P., 2004. Reduction and oxidation kinetics of a copper-based oxygen carrier prepared by impregnation for chemical-looping combustion. Ind. Eng. Chem. Res. 43 (26), 8168–8177.
Gonzalez, B., Blamey, J., McBride-Wright, M., Carter, N., Dugwell, D., Fennell, P., Abanades, J.C., 2011. Calcium looping for CO_2 capture: sorbent enhancement through doping. Energy Procedia 4, 402–409.
Grasa, G.S., Abanades, J.C., 2006. CO_2 capture capacity of CaO in long series of carbonation/calcinations cycles. Ind. Eng. Chem. Res. 45, 8846–8851.
Grasa, G.S., Abanades, J.C., Alonso, M., Gonzalez, B., 2008. Reactivity of highly cycled particles of CaO in a carbonation/calcination loop. Chem. Eng. J. 137 (3), 561–567.
Hossain, M.M., de Lasa, H.I., 2008. Chemical-looping combustion (CLC) for inherent CO_2 separations – a review. Chem. Eng. Sci. 63, 4433–4451.
IEA, 2008. CO_2 Capture in the Cement Industry, July 2008/3.
IEA, 2009a. World Energy Outlook 2009, http://www.worldenergyoutlook.org/publications/weo-2009/.
IEA, 2009b. Carbon emission reductions up to 2050. In: Cement Technology Roadmap 2009.
IEA, 2010. Energy Technology Perspectives 2010: Scenarios & Strategies to 2050, Paris, France.
IEA, 2012. CCS Retrofit: Analysis of the Globally Installed Coal-Fired Power Station Fleet. OECD/IEA, Paris, France.
IEAGHG, 2009. Biomass CCS Study: Techno-Economic Evaluation of Biomass Fired or Co-Fired Power Plant with Post-Combustion CO_2 Capture. IEAGHG, Cheltenham, UK.
IEAGHG, 2014. CO_2 Capture at Coal Based Power and Hydrogen Plants, May 2014/3.
IPCC, 2013. Climate Change 2013: The Physical Science Basis. In: Stocker, T.F., Qin, D., Plattner, G.K., Tignor, M., Allen, S.K., Boschung, J., Nauels, A., Xia, Y., Bex, V., Midgley, P.M. (Eds.), Contribution of Working Group I to the Fifth Assessment Report of the Intergovernmental Panel on Climate Change. Cambridge University Press, Cambridge, United Kingdom/New York, NY, USA, p. 1535, http://dx.doi.org/10.1017/CBO9781107415324.
Ishida, M., Jin, H., 1994. A new advanced power-generation system using chemical-looping combustion. Energy 19 (4), 415–422.
Imtiaz, Q., Kierzkowska, A.M., Müller, C.R., 2012. Coprecipitated, copper-based, alumina-stabilized materials for carbon dioxide capture by chemical looping combustion. ChemSusChem 5 (8), 1610–1618.
Imtiaz, Q., Hosseini, D., Müller, C.R., 2013. Review of oxygen carriers for chemical looping with oxygen uncoupling (CLOU): thermodynamics, material development, and synthesis. Energy Technol. 1 (11), 633–647.
Jared, C.P., Sean, P.I., Lynn, B., Andrew, J., Gregson, V., Shiaoguo, C., 2010, September. DOE/NETL Advanced Carbon Dioxide Capture R&D Program: Technology Update.
Kierzkowska, A.M., Müller, C.R., 2012. Development of calcium-based, copper-functionalised CO_2 sorbents to integrate chemical looping combustion into calcium looping. Energy Environ. Sci. 5, 6061–6065.
Kierzkowska, A.M., Müller, C.R., 2013. Sol–gel derived, calcium-based, copper-functionalised CO_2 sorbents for an integrated chemical looping combustion-calcium looping CO_2 capture process. ChemPlusChem 78, 92–100.
Kierzkowska, A.M., Pacciani, R., Müller, C.R., 2013. CaO-based CO_2 sorbents: from fundamentals to the development of new, highly effective materials. ChemSusChem 6 (7), 1130–1148.
Kolovos, K., Barafaka, S., Kakali, G., Tsivilis, S., 2005. CuO and ZnO addition in the cement raw mix: effect on clinkering process and cement hydration and properties. Ceramics 49, 205–212.
Kremer, J., Galloy, A., Ströhle, J., Epple, B., 2013. Continuous CO_2 capture in a 1-MW_{th} carbonate looping pilot plant. Chem. Eng. Technol. 36 (9), 1518–1524.
Kunii, D., Levenspiel, O., 1991. Fluidization Engineering, second ed. Butterworth-Heinemann, Boston.
Li, Z.S., Cai, N.S., Croiset, E., 2008. Process analysis of CO_2 capture from flue gas using carbonation/calcination cycles. AIChE J. 54 (7), 1912–1925.
Linnhoff, B., Flower, J.R., 1978. Synthesis of heat exchanger networks: I. Systematic generation of energy optimal networks. AIChE J. 24 (4), 633–642.
Lu, H., Reddy, E.P., Smirniotis, P.G., 2006. Calcium oxide based sorbents for capture of carbon dioxide at high temperatures. Ind. Eng. Chem. Res. 45, 3944–3949.
Lu, D.Y., Hughes, R.W., Anthony, E.J., 2008. Ca-based sorbent looping combustion for CO_2 capture in pilot-scale dual fluidized beds. Fuel Process. Technol. 89 (12), 1386–1395.
Lyon, R.K., Cole, J.A., 2000. Unmixed combustion: an alternative to fire. Combust. Flame 121, 249–261.
Manovic, V., Anthony, E.J., 2011a. Reactivation and remaking of calcium aluminate pellets for CO_2 capture. Fuel 90 (1), 233–239.
Manovic, V., Anthony, E.J., 2011b. CaO-based pellets with oxygen carriers and catalysts. Energy Fuels 25 (10), 4846–4853.
Manovic, V., Wu, Y., He, I., Anthony, E.J., 2011c. Core-in-shell CaO/CuO-based composite for CO_2 capture. Ind. Eng. Chem. Res. 50, 12384–12391.
Manovic, V., Anthony, E.J., 2011d. Integration of calcium and chemical looping combustion using composite CaO/CuO-based materials. Environ. Sci. Technol. 45, 10750–10756.
Martinez, I., Romano, M.C., Fernández, J.R., Chiesa, P., Murillo, R., Abanades, J.C., 2014. Process design of a hydrogen production plant from natural gas with CO_2 capture based on a novel Ca/Cu chemical loop. Appl. Energy 114, 192–208.
McCauley, K.J., Farzan, H., Alexander, K.C., McDonald, D.K., 2009. Commercialization of oxy-coal combustion: applying results of a large 30 MW_{th} pilot project. Energy Procedia 1, 439–446.
Merkel, T.C., Lin, H., Wei, X., Baker, R., 2010. Power plant post-combustion carbon dioxide capture: an opportunity for membranes. J. Membr. Sci. 359 (1), 126–139.
Olivier, J.G., Janssens-Maenhout, G., Muntean, M., Peters, J.A., 2013. Trends in Global CO_2 Emissions 2013 Report. PBL Netherlands Environmental Assessment Agency.
Ozcan, D.C., Shanks, B.H., Wheelock, T.D., 2011. Improving the stability of a CaO-based sorbent for CO_2 by thermal pretreatment. Ind. Eng. Chem. Res. 50 (11), 6933–6942.
Ozcan, D.C., Ahn, H., Brandani, S., 2013. Process integration of a Ca-looping carbon capture process in a cement plant. Int. J. Greenh. Gas Control 19, 530–540.
Ozcan, D.C., Alonso, M., Ahn, H., Abanades, J.C., Brandani, S., 2014. Process and cost analysis of a biomass power plant with in situ calcium looping CO_2 capture process. Ind. Eng. Chem. Res. 53 (26), 10721–10733.
Qin, C., Yin, J., Liu, W., An, H., Feng, B., 2012. Behavior of CaO/CuO based composite in a combined calcium and copper chemical looping process. Ind. Eng. Chem. Res. 51, 12274–12281.
Qin, C., Yin, J., Luo, C., An, H., Liu, W., Feng, B., 2013. Enhancing the performance of CaO/CuO based composite for CO_2 capture in a combined Ca–Cu chemical looping process. Chem. Eng. J. 228, 75–86.
Rao, A.B., Rubin, E.S.A., 2002. Technical, economic, and environmental assessment of amine-based CO_2 capture technology for power plant greenhouse gas control. Environ. Sci. Technol. 36, 4467–4475.
Rodriguez, N., Alonso, M., Abanades, J.C., 2010. Average activity of CaO particles in a calcium looping system. Chem. Eng. J. 156 (2), 388–394.
Rodriguez, N., Murillo, R., Alonso, M., Martinez, I., Grasa, G., Abanades, J.C., 2011. Analysis of a process for capturing the CO_2 resulting for pre-calcination of limestone in a cement plant. Ind. Eng. Chem. Res. 50 (4), 2126–2132.
Rodriguez, N., Murillo, R., Abanades, J.C., 2012. CO_2 capture from cement plants using oxyfired precalcination and/or calcium looping. Environ. Sci. Technol. 46 (4), 2460–2466.
Romano, M.C., 2012. Modeling the carbonator of a Ca-looping process for CO_2 capture from power plant flue gas. Chem. Eng. Sci. 69 (1), 257–269.
Romano, M.C., Martinez, I., Murillo, R., Arstad, B., Blom, R., Ozcan, D.C., Ahn, H., Brandani, S., 2012. Guidelines for Modeling and Simulation of Ca-looping Processes, EERA CCS Report.
Romeo, L.M., Abanades, J.C., Escosa, J.M., Pano, J., Gimenez, A., 2008. Oxyfuel carbonation/calcination cycle for low cost CO_2 capture in existing power plants. Energy Convers. Manage. 49, 2809–2814.

Shimizu, T., Hirama, T., Hosoda, H., Kitano, K., Inagaki, M., Tejima, K., 1999. A twin fluid-bed reactor for removal of CO_2 from combustion processes. Chem. Eng. Res. Des. 77, 62–68.

Telesca, A., Calabrese, D., Marroccoli, M., Tomasulo, M., Valenti, G.L., Montagnaro, F., 2014. Spent limestone sorbent from calcium looping cycle as a raw material for the cement industry. Fuel 118, 202–205.

Tobiesen, F.A., Juliussen, O., Svendsen, H.F., 2008. Experimental validation of a rigorous desorber model for CO_2 post-combustion capture. Chem. Eng. Sci. 63 (10), 2641–2656.

U. K. Parliament (UKP), 2008. Climate Change Act 2008, London, UK.

Xu, G., Li, L., Yang, Y., Tian, L., Liu, T., Zhang, K., 2012. A novel CO_2 cryogenic liquefaction and separation system. Energy 42 (1), 522–529.